Effect of CO2 on shale caprock integrity – shale exposure experiments

Ife

Institute for Energy Technology

Report number	Availability	Revision number	Date
IFE/KR/F-2015/087	CONFIDENTIAL		2015-06-22
Client/ Client reference:	Availability this page CONFIDENTIAL	Number of issues	Number of pages 25

Report title

Effect of CO2 on shale caprock integrity – shale exposure experiments

Summary

Shale is an important caprock overlying numerous geological reservoirs considered for CO_2-storage. Therefore, it is important to determine whether chemical and physical interactions between shales and the injected CO_2 can impact he sealing integrity of this caprock, and hence the reservoir storage capacity. During CO_2-storage, the shale caprock mainly comes into contact with the supercritical CO_2 bubble, rather than with CO_2 dissolved in water. Therefore, possible physical and chemical interactions between dry or wet supercritical CO_2 and the minerals plus any organic matter present in the caprock need to be determined, as well as the effects that these interactions may have on shale caprock integrity.

Whereas mineralogical changes were not observed during direct exposure of various pure minerals to supercritical CO_2, the exposure of natural, multi-component shale samples may result in changes to the kerogen contained in these shales, as well as other effects. Therefore, we have carried out experiments in which shale rock samples, either ~1 gr of powdered shale, or ~1 cm3 shale cuboids, were exposed to dry and hydrous supercritical CO_2 in 60 ml batch vessels, at a temperature of 40°C and a pressure of up to 10 MPa. X-ray Diffraction (XRD) and Thermo-Gravimetric Analysis (TGA) were used on the powdered shales to determine whether any significant enduring changes to the shale composition occurred. Optical methods were used to distinguish effects of exposure to CO_2 on shale (micro-)structure after the experiments on intact pieces of shale.

Distribution

Electronic:

Paper:

File (x copies)

Library (1 copy)

	Name	Signature
Prepared by	Reinier van Noort	
Reviewed by	Magnus Wangen	
Approved by	Nina Simon	

Electronic file code

Contents

1   Introduction

The caprocks over many reservoirs considered for CO_2-storage, including Sleipner, Snøhvit, and Longyearbyen consist of layers of shale. Therefore, chemical and physical interactions between shale caprocks and supercritical CO_2 can have a large impact on the integrity of the seal, and on the reservoir storage capacity [1][2].

Chemical reactions between dissolved CO_2, shale and water have previously been studied (e.g., [1][2][3][4]). Laboratory studies have shown that interaction with dry supercritical CO_2 may lead to the dehydration of clay minerals. Alternatively, uptake of CO_2 may result in swelling of clay minerals under certain circumstances ([5][6][7]). When swelling occurs in shale under confined conditions, this could result in stress generation, pore closure, and/or cracking. Dehydration could result in shrinkage and crack generation. Therefore, these processes can have a large impact on the permeability of shale caprocks. Additionally, interaction with supercritical CO_2 may result in the release of hydrocarbons from organic-rich shales. This may further influence the integrity of the shale seal, and can also be of interest for enhanced oil recovery by CO_2-injection.

In this report, two sets of experiments studying the interaction between supercritical CO_2 and shale will be discussed. Initially, a preliminary set of experiments was carried out by Souche, and finished before May 2013 (see [8]). These preliminary experiments include experiments performed on powdered shale, powdered shale compacted to tablets, and cm-scale pieces of intact shale rock. A second set of experiments was initiated in September 2014 by the present author.

2 Methods

2.1 Sample selection and preparation

For the preliminary experiments, two shale samples, 25/5 1/M1 and 25/5 1M9, were selected based on the shale compositions analyzed using XRD and RockEval pyrolysis, as reported in ([9] – see **Table 1**. Shale compositions. for compositions of selected samples). Shale sample 25/5 1/M1 was selected based on its high smectite/illite ratio in the mixed layer phase of 0.70. Shale sample 25/5 1/M9 was selected for its high kaolinite content (no smectite). Both samples come from the same borehole (25/5 1), but from different depths (2917.5 and 3279.4 m respectively).

For the second series of experiments, a third sample, 25/5 1/M4, was selected, based on its high overall clay content and the amount of sample available. This sample originates from the same borehole, at a depth of 3042.5 m.

A powdered sample of 25/5 1/M1 was prepared by crushing of representative pieces in a percussion mortar, followed by sieving over a 450 µm sieve, and further crushing of the coarser fragments. A finely powdered sample was acquired by wet micronizing a fraction of the powdered sample in a McCrone micronizing mill with agate grinding elements for 10 minutes. Presumably this was done in water. The resulting slurry was filtered over a 0.45 µm filter, dried overnight, and then lightly crushed using a mortar[8].

A finely powdered sample of 25/5 1/M4 was prepared by grinding representative pieces of the material in an agate ball mill, sieving off all fragments coarser than 20 µm, and re-grinding these fragments until all material passed through the 20 µm sieve. An additional powdered sample was acquired by micronizing, following the method described above.

For experiments performed on pieces of shale, representative parts were selected from the available material, and cut to size using a diamond saw. It is unknown whether the fragments used in the preliminary experiments (carried out by [8]) were cut wet or dry. The fragments cut for the second series of experiments were cut dry, i.e. without water or cutting fluids, using a fine circular saw. During cutting, care was taken to prevent heating of the samples. For the second series experiment on a piece of 25/5 1/M1 shale (RN-B-06), the only available large piece was used.

2.2 Batch vessels

All experiments discussed here were carried out in Hastelloy C batch vessels, each with an internal volume of 60 ml. Each batch vessel was equipped with a PTX 1400 pressure transmitter, and a shielded K-type thermocouple located near the bottom of the vessel for temperature control. The vessels were heated using heating jackets placed around the outside of the vessels. These jackets allowed the temperature to be controlled to within ± 0.2°C. Pressurization and depressurization took place via a needle valve connected to a port in the lid of each vessel. An ISCO Syringe-pump was used to reach the required CO_2-pressure. During the preliminary powder experiment, a magnetic stirring rod was employed to stir the contents of the vessel. The vessels were sealed by a Teflon O-ring. During the tests, the temperature and pressure in each vessel were logged using an Agilent 34970A Data logger connected to a personal computer.

The following description of the procedure used to set up an experiment is only valid for the second series of experiments. No information is available on the procedure used for the preliminary experiments. When setting up an experiment, first the sample to be used was carefully measured. In the case of powder samples, a pre-determined mass of sample was measured and placed inside the vessel. In the case of samples consisting of larger pieces of shale rock, the dimensions of the samples, as well as their mass were determined. Next, the sample was loaded into the vessel. The vessel was then sealed and flushed three times with CO_2, by filling it with CO_2, typically to a pressure of ~1 MPa, then releasing the pressure in a controlled manner. After flushing, the vessel was pressurized to a lower pressure than the final experimental pressure, the needle valve on the vessel was closed, and temperature-control was switched on. During heating, if the pressure increased beyond the desired value, the excess CO_2 was carefully bled-off. Once the temperature was stable at the desired value, the vessel was pressurized to the desired operational pressure, and the needle valve was closed, thus starting the experiment.

At the end of each experiment, the temperature control was switched off, and the vessel rapidly cooled to room temperature. At close to room temperature, the pressure on the vessel was carefully released through the needle valve, preventing rapid depressurization. Once depressurized, the vessel was opened and the sample recovered. TGA and XRD analyses were carried out as quickly as possible after the vessel was depressurized, though typically, up to two hours might pass between depressurization and initialization of all analyses.

In most experiments, the pressure did not vary by more than ± 2%. During some experiments the pressure decreased slowly as a result of minor leaks in our experimental setup. When this occurred, the pressure was increased back to the desired value regularly to prevent the pressure from decreasing by more than 10% from the set value.

A list of all experiments reported here is provided in Table 2. A list of all reported experiments..

2.3   Sample characterization

Sample characterization was performed using optical methods, Thermo-Gravimetric Analysis (TGA), X-Ray diffraction (XRD), and Scanning Electron Microscopy (SEM), on both untreated and reacted samples, in order to detect chemical and physical changes in the shale samples resulting from interactions with (supercritical) CO_2.

TGA was performed in the custom-built TGA system at IFE environmental technology, with a heating rate of either 1°C per minute for the preliminary measurements, or 2°C per minute for the later measurements, under a flow of N_2. Additional TG Analyses were carried out at IFE in a Netzsch STA 449F3 TGA/DSC under a flow or Ar.

XRD analysis was performed using a Bruker D8 Advance diffractometer (Cu-K1, radiation) equipped with a one-dimensional PSD (LynxEye) detector.

Table 1. *Shale compositions.*

Sample #	25/5 1/M1	25/5 1/M4	25/5 1/M9
Formation	Draupne	Tarbert	Statfjord
10Å Physil	2,7	11,9	3,8
7Å Physil	7,4	17,0	56,3
4.7Å Physil	0,0	1,7	0,0
Quartz	52,9	48,3	31,4
Alkali Feldspar	0,7	4,8	1,9
Plagioclase	1,8	2,0	3,3
TiOx	1,7	0,0	0,0
Calcite	0,6	0,0	0,0
Dolomite / Ankerite	7,8	0,3	0,0
Siderite	1,7	9,4	1,7
Pyrite	22,1	4,7	1,6
Gypsum	0,7	0,0	0,0
toc	6,2	6,6	13,6

Table 2. *A list of all reported experiments.*

Preliminary experiments						
	Sample	Dur (d)	M (g)	T (°C)	P (MPa)	Notes.
AS-P-01	M1	14	~1.5	30	7	Fine powder (micronised 25/5 1/M1).
AS-B-02	M1 M9	14	- -	30	7.5	Two rough cut cuboid or near-cuboid blocks of shale, samples 25/5 1/M1 and 25/5 1/M9.
Second series experiments						
	Sample	Dur (d)	M (g)	T (°C)	P (MPa)	Notes.
RN-P-01	M1	14	0.9990	40	10	Fine powder (micronised 25/5 1/M1).
RN-P-02	M1	19	0.9998	30	7	Fine powder (micronised 25/5 1/M1).
RN-P-03	M4	14	1.0000	40	10	Fine powder (ball-milled 25/5 1/M4).
RN-B-04	M4	8	2.5286	40	10	Rough ~1 cm3 cuboid block of shale.
RN-B-05	M4	14	2.8930	40	10	Rough ~1 cm3 cuboid block of shale.
RN-B-06	M1 M9	9	6.052 5.537	40	10	Two rough cut cuboid blocks of shale, samples 25/5 1/M1 and 25/5 1/M9.
RN-P-07	M1	14	0.6750	40	10	Fine powder (micronised 25/5 1/M1). Small amount (~0,072 gr) of water added to sample.
RN-P-08	M4	14	0.9985	40	10	Fine powder (micronised 25/5 1/M4), 5.933 gr H2O added, separated from sample.
RN-P-09	M4	14	0.9990	40	10	Fine powder (micronised 25/5 1/M4) and stirring.
RN-P-10	M4	14	0.9995	80	10	Fine powder (micronised 25/5 1/M4), higher T.
RN-P-11	M4	15	1.0002	40	10	Fine powder (micronised 25/5 1/M4), argon and stirring.
RN-P-12	M4	14	0.9995	40	10	Fine powder (micronised 25/5 1/M4), stirring with commercially acquired neodymium magnets.
RN-B-13	M4	14	11.4439	40	11	Moistened rough ~5cm3 cuboid block of shale.

3 Results

3.1 Starting material characterization

3.1.1 TGA on starting materials

An initial TG Analysis of micronized 25/5 1/M1 showed rapid mass loss at temperatures up to 80°C, much slower mass loss between 80°C and 390°C, and then more rapid mass loss again up to 640°C. The total mass loss measured in the unreacted sample was ~8.5% of the starting mass (see Figure 1. Mass loss vs. temperature plots from analyses performed on the IFE TGA system. Starting material 25/5 1/M1 and experiments (a) AS-P-01 (analyses by Souche, 2013), and (b) RN-P-01 and RN-P-02.a).

A repeat analysis on the same sample showed an initial rapid decrease in mass up to ~90°C, followed by slower mass loss up to ~380°C, and then another period of increased mass loss up to 610°C. The sample mass was still decreasing slowly when the maximum temperature of 700°C was reached. The maximum decrease in mass measured was ~12.9% (see Figure 1. Mass loss vs. temperature plots from analyses performed on the IFE TGA system. Starting material 25/5 1/M1 and experiments (a) AS-P-01 (analyses by Souche, 2013), and (b) RN-P-01 and RN-P-02.b).

A second repeat analysis, performed on the 25/5 1/M1 starting material using the Netzsch TGA similarly showed limited initial mass loss up to 110°C, near constant mass between 110°C and 350°C, and rapid mass loss between 350°C and 620°C (Figure 2. TG Analyses performed on the Netzsch TGA, showing (a) a plot of remaining sample mass (%) vs. temperature (°C), and (b) a plot of the rate of mass loss (%/min) vs. temperature (°C), for the 25/5 1/M1 starting material, and samples exposed to (near-)supercritical CO_2 in experiments AS-P-01 and RN-P-07.a). A plot of the rate of mass loss (in % / min., averaged over 10 minute intervals – see Figure 2. TG Analyses performed on the Netzsch TGA, showing (a) a plot of remaining sample mass (%) vs. temperature (°C), and (b) a plot of the rate of mass loss (%/min) vs. temperature (°C), for the 25/5 1/M1 starting material, and samples exposed to (near-)supercritical CO_2 in experiments AS-P-01 and RN-P-07.b) shows four distinct peaks in the mass loss rate between 300°C and 620°C, the first and largest between 320°C and 465°C, the second between 465°C and 510°C and the last two smaller peaks between 510°C and 620°C. Note that the temperature at which each transition occurs is sensitive to both the apparatus and the settings used.

The TG Analysis performed on powdered 25/5 1/M4 starting material (in the Netzsch TG Analyzer – see Figure 3. TG Analyses performed on the Netzsch TGA, showing (a) a plot of remaining sample mass (%) vs. temperature (°C), and (b) a plot of the rate of mass loss (%/min) vs. temperature (°C), for the 25/5 1/M4 starting material, and samples exposed to supercritical CO_2 or argon in experiments RN-P-03, RN-P-09, RN-P-10, RN-P-11 and RN-P-12.a) shows mass loss at lower temperature (below 130°C) followed by a period of near-constant mass up to 330°C, rapid mass loss between 330°C and 480°C, ongoing slower mass loss between 480°C and 700°C, and finally somewhat more rapid mass loss up to 800°C. The mass loss rate plot (averaged over 10 minutes – see Figure 3. TG Analyses performed on the Netzsch TGA, showing (a) a plot of remaining sample mass (%) vs. temperature (°C), and (b) a plot of the rate of mass loss (%/min) vs. temperature (°C), for the 25/5 1/M4 starting material, and samples exposed to supercritical CO_2 or argon in

experiments RN-P-03, RN-P-09, RN-P-10, RN-P-11 and RN-P-12.b) shows a single large peak between 330°C and 480°C and a smaller peak between 700°C and 800°C.

3.1.2   XRD on starting materials

New XRD analyses on the starting materials were primarily performed in order to confirm the samples were still usable, and to be able to detect changes in the XRD spectra after each experiment (see Figure 4. XRD analyses. (a) Starting material 25/5 1/M1, reacted material AS-P-01, and reacted material AS-P-01 after TGA. (b) Starting material 25/5 1/M1, reacted materials AS-P-01, RN-P-01, RN-P-02 and RN-P-07. (c) starting material 25/5 1/M4 and reacted materials RN-P-03, RN-P-09, RN-P-10, RN-P-11 and RN-P-12.). New quantitative analyses were not performed as such analyses were available from an earlier project ([9] – see also **Table 1**. Shale compositions. for relevant compositions). The main diffraction peaks related to clay minerals were observed for layer spacings of 7 and 10 Å. A minor, broad bulge was observed around 14 Å.
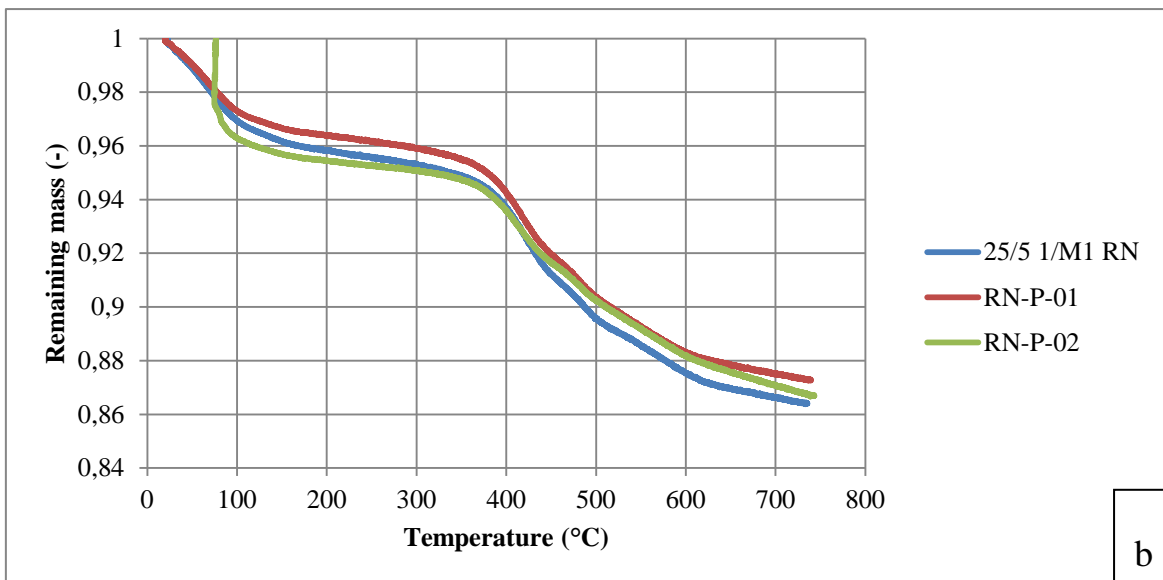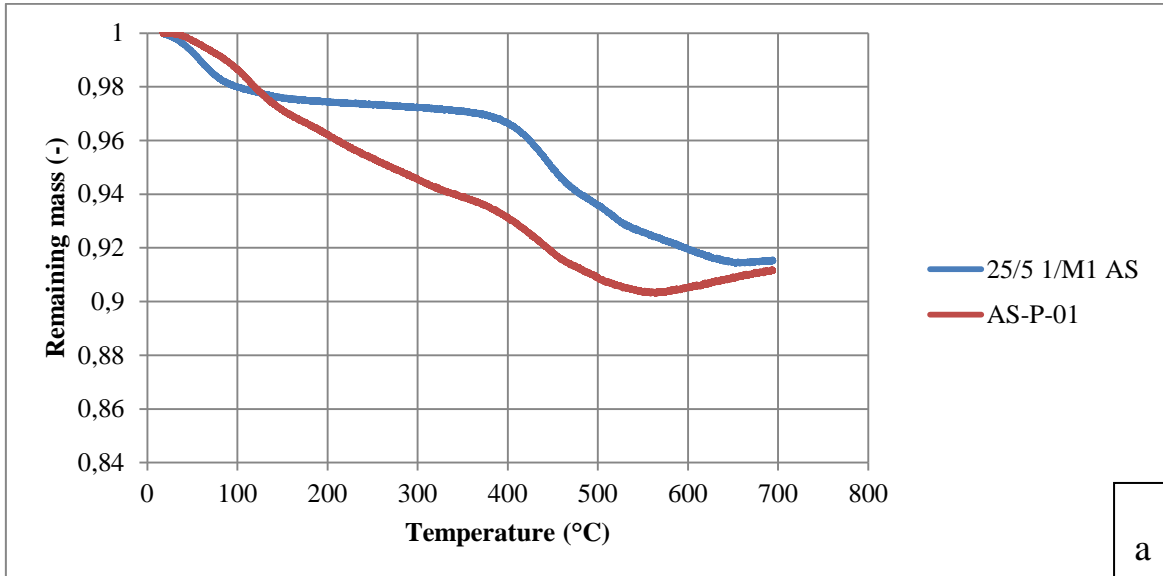
Figure 1. *Mass loss vs. temperature plots from analyses performed on the IFE TGA system. Starting material 25/5 1/M1 and experiments (a) AS-P-01 (analyses by Souche, 2013), and (b) RN-P-01 and RN-P-02.*
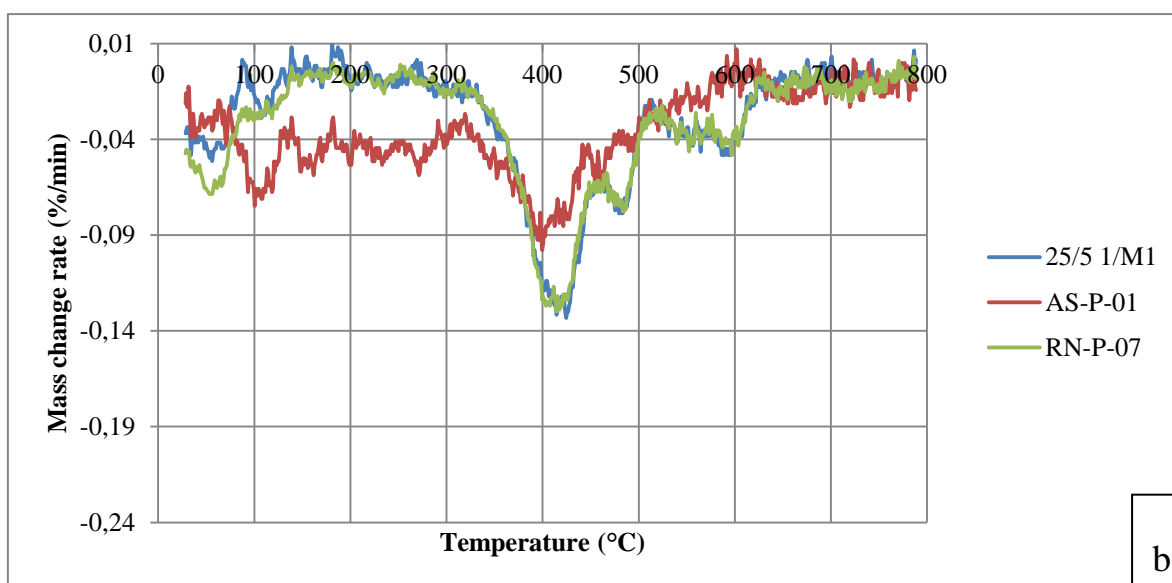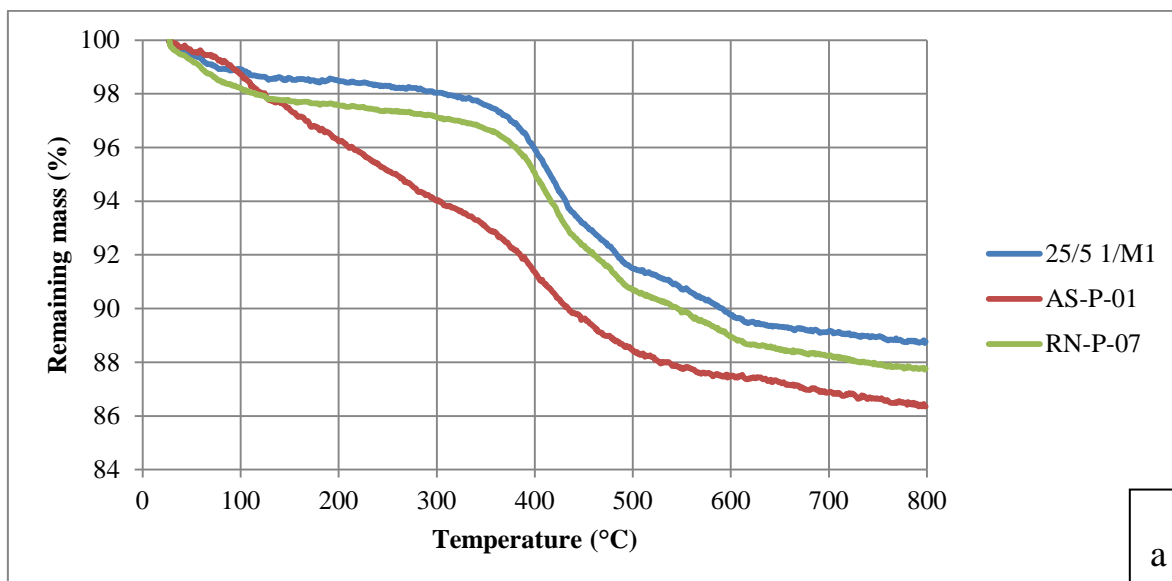
Figure 2. *TG Analyses performed on the Netzsch TGA, showing (a) a plot of remaining sample mass (%) vs. temperature (°C), and (b) a plot of the rate of mass loss (%/min) vs. temperature (°C), for the 25/5 1/M1 starting material, and samples exposed to (near-)supercritical CO_2 in experiments AS-P-01 and RN-P-07.*
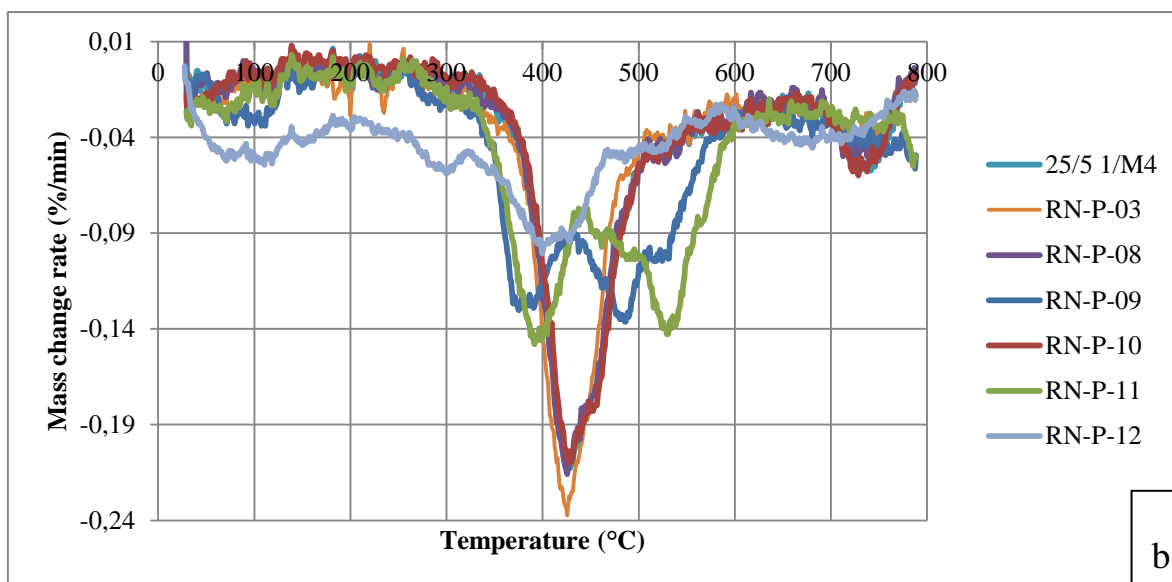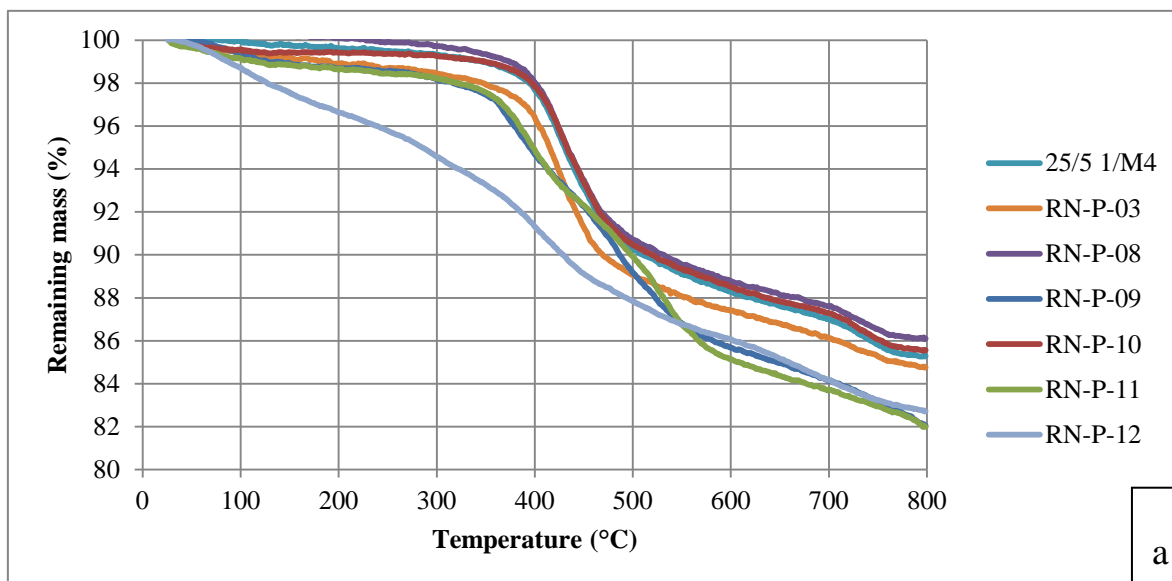
Figure 3. *TG Analyses performed on the Netzsch TGA, showing (a) a plot of remaining sample mass (%) vs. temperature (°C), and (b) a plot of the rate of mass loss (%/min) vs. temperature (°C), for the 25/5 1/M4 starting material, and samples exposed to supercritical CO2 or argon in experiments RN-P-03, RN-P-09, RN-P-10, RN-P-11 and RN-P-12.*
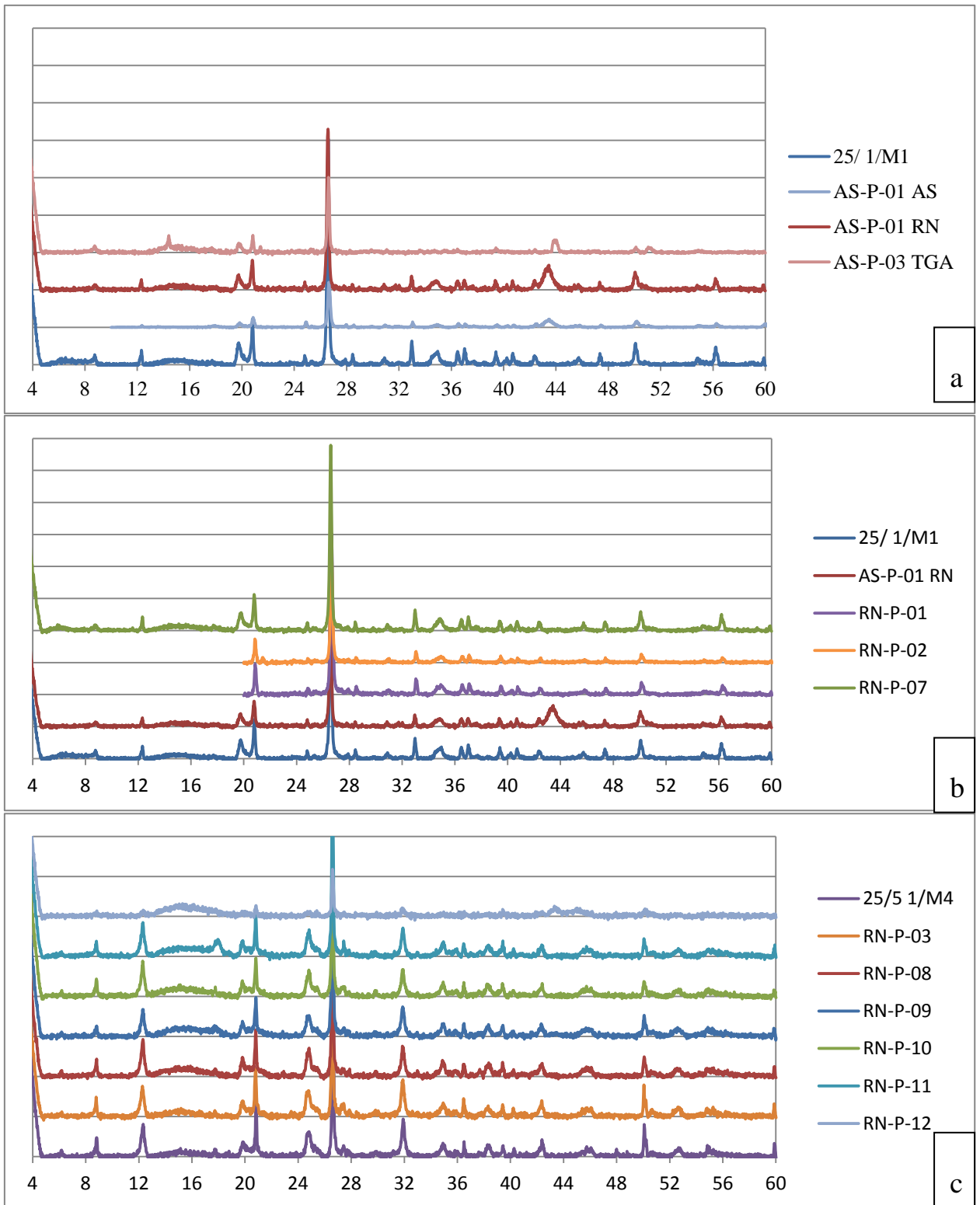
Figure 4. XRD analyses. (a) Starting material 25/5 1/M1, reacted material AS-P-01, and reacted material AS-P-01 after TGA. (b) Starting material 25/5 1/M1, reacted materials AS-P-01, RN-P-01, RN-P-02 and RN-P-07. (c) starting material 25/5 1/M4 and reacted materials RN-P-03, RN-P-09, RN-P-10, RN-P-11 and RN-P-12.

3.2 Preliminary experiments

3.2.1 Powder experiment AS-P-01

Souche [8] reports one experiment on micronized 25/5 1/M1 shale. After ending the experiment, the powder had agglomerated into lumps and its color was somewhat lighter grey than the starting material. TGA and XRD analyses were performed on the reacted powder, but it is unknown how soon after the experiment these tests were executed.

The TG Analysis of the reacted powder (see Figure 1. Mass loss vs. temperature plots from analyses performed on the IFE TGA system. Starting material 25/5 1/M1 and experiments (a) AS-P-01 (analyses by Souche, 2013), and (b) RN-P-01 and RN-P-02.a) showed continuous mass loss up to 570°C at a near constant rate, though a slight decrease in rate is observed at 130°C and a slight increase is observed at 390°C, comparable to the changes in rate in the unreacted sample. At temperatures above ~570°C, the reacted sample shows an increase in mass. The reacted sample showed a maximum mass loss of ~9.7%.

A repeat analysis performed on the Netzsch STA 449F3 performed more than a year after the experiment showed a similar pattern with constant mass loss up to 350°C, followed by somewhat more rapid mass loss between 350°C and 550°C (Figure 2. TG Analyses performed on the Netzsch TGA, showing (a) a plot of remaining sample mass (%) vs. temperature (°C), and (b) a plot of the rate of mass loss (%/min) vs. temperature (°C), for the 25/5 1/M1 starting material, and samples exposed to (near-)supercritical CO_2 in experiments AS-P-01 and RN-P-07.a). A plot of the rate of mass loss (in % / min., averaged over 10 minute intervals – see Figure 2. TG Analyses performed on the Netzsch TGA, showing (a) a plot of remaining sample mass (%) vs. temperature (°C), and (b) a plot of the rate of mass loss (%/min) vs. temperature (°C), for the 25/5 1/M1 starting material, and samples exposed to (near-)supercritical CO_2 in experiments AS-P-01 and RN-P-07.b) shows a peak between 70°C and 120°C, a large peak between 320°C and 445°C, and a peak between 445°C and 600°C. A further minor peak is observed between 625°C and 715°C.

The XRD spectrum of the reacted sample is very comparable to the spectrum of the starting material (Figure 4. XRD analyses. (a) Starting material 25/5 1/M1, reacted material AS-P-01, and reacted material AS-P-01 after TGA. (b) Starting material 25/5 1/M1, reacted materials AS-P-01, RN-P-01, RN-P-02 and RN-P-07. (c) starting material 25/5 1/M4 and reacted materials RN-P-03, RN-P-09, RN-P-10, RN-P-11 and RN-P-12.a). However, the reacted sample showed the appearance of one new significant peak at ~43° (2,10Å). A re-analysis of the reacted sample performed over a year after ending the experiment confirmed that this peak was still present, suggesting a non-transient change in the mineral phases present in the sample. Furthermore, the broad bulge around 14Å observed in the starting material was not present in the reacted sample (in both analyses). An XRD analysis was also performed on the reacted sample after TGA (see Figure 4. XRD analyses. (a) Starting material 25/5 1/M1, reacted material AS-P-01, and reacted material AS-P-01 after TGA. (b) Starting material 25/5 1/M1, reacted materials AS-P-01, RN-P-01, RN-P-02 and RN-P-07. (c) starting material 25/5 1/M4 and reacted materials RN-P-03, RN-P-09, RN-P-10, RN-P-11 and RN-P-12.a).

3.2.2 Shale block experiment AS-B-02

In this experiment, two cm-scale blocks of shale were placed inside a batch vessel and reacted with CO_2 at 30°C and 7.5 MPa for two weeks. One block was cut from sample 25/5

1/M1, and the other from sample 25/5 1/M9. After the experiment, the 25/5 1/M1 block looked dried out and had split along some of its layers, whereas the 25/5 1/M9 block appeared wet, and had remained intact. Furthermore, upon opening the vessel, the M9 sample was releasing fluids, which appeared to be rich in hydrocarbons, based on fluorescence [8].

3.3 Second series of experiments

3.3.1 Powder experiments RN-P-01, RN-P-02 and RN-P-07

The initial purpose of the second set of experiments was to reproduce the results obtained in the preliminary experiments. Upon successful reproduction of the initial results, further experiments would be planned, based on these results.

Experiment RN-P-01 was aimed at directly reproducing the results reported for experiment AS-P-01, except that a slightly higher temperature and pressure were chosen to ensure that the CO_2 would be in supercritical state. Furthermore, a smaller sample was used to preserve the limited available material, and the experiment was not stirred. After the experiment was finished, the sample was studied optically, and XRD and TG analyses were started as quickly as possible, within 2 hours.

Optical inspection showed no significant change to the powder. As much sample as possible was recovered from the vessel. The total mass of the recovered sample was 0.9790 g (starting mass 0.9990 g), but during depressurization the powder was spread throughout the reaction vessel (and possibly carried into the pipework as well). After a further resting period of 10 minutes, the recovered mass had decreased to 0.9764, most likely as a result of further degassing of CO_2 from the powder.

A second experiment, RN-P-02 was carried out with a pressure of 7 MPa and a temperature of 30°C to more closely reproduce the conditions of experiment AS-P-01. Again, the experiment was not stirred. After the experiment, the sample was once again spread throughout the vessel, but the total sample mass recovered was 1.0070 g (0.9998 g starting mass). Other than that, the sample showed some clumping, but no further changes.

In the third powder experiment performed on 25/5 1/M1 powder, RN-P-07, a small amount of water (~0.072 g, approximately the amount that would be expected to dissolve in the available supercritical CO_2 under experimental conditions) was added to the powder before the vessel was closed. This was done in order to determine if small amounts of water that might have been present in the earlier (first series) experiments would have influenced the reactions that might take place. Upon opening the vessel, the powder looked somewhat clumped, and it was noted that a layer of powder was attached to the bottom of the vessel. Loose powder had also spread throughout the vessel. Of the initial sample mass of 0.6750 g, 0.6224 g was recovered.

TG Analysis of RN-P-01 on the IFE analyzer (Figure 1. Mass loss vs. temperature plots from analyses performed on the IFE TGA system. Starting material 25/5 1/M1 and experiments (a) AS-P-01 (analyses by Souche, 2013), and (b) RN-P-01 and RN-P-02.b) showed a very similar pattern to the most recent analysis of the unreacted sample performed on the same analyzer, except that the initial period of rapid mass loss (slowing down from 90°C to ~160°C) resulted in a decrease in mass of only 3.4% rather than 3.7% (relative to the starting mass). The total measured mass loss of sample RN-P-01 was ~12.5%.

TG Analysis of RN-P-02 (Figure 1. Mass loss vs. temperature plots from analyses performed on the IFE TGA system. Starting material 25/5 1/M1 and experiments (a) AS-P-01 (analyses by Souche, 2013), and (b) RN-P-01 and RN-P-02.b) showed a somewhat larger decrease in mass after the initial rapid period of mass loss (4.4% at 160°C), and a larger total decrease in mass at peak temperature (700°C) of 13.3%. Note that due to time restrictions and the slow cooling rate of the TGA used, this analysis was started at a relatively high initial temperature, which causes an initial very rapid drop in sample mass.

TG Analysis of RN-P-07, performed on the Netzsch STA 449F3 showed a very similar mass loss pattern to that observed on the starting material in the same apparatus (see Figure 2. TG Analyses performed on the Netzsch TGA, showing (a) a plot of remaining sample mass (%) vs. temperature (°C), and (b) a plot of the rate of mass loss (%/min) vs. temperature (°C), for the 25/5 1/M1 starting material, and samples exposed to (near-)supercritical CO2 in experiments AS-P-01 and RN-P-07.a), with rapid mass loss occurring between 350°C and 620°C. An analysis of the rate of mass loss (%/min. averaged over 10 minute intervals, see Figure 2. TG Analyses performed on the Netzsch TGA, showing (a) a plot of remaining sample mass (%) vs. temperature (°C), and (b) a plot of the rate of mass loss (%/min) vs. temperature (°C), for the 25/5 1/M1 starting material, and samples exposed to (near-)supercritical CO2 in experiments AS-P-01 and RN-P-07.b) again shows four distinct peaks, the largest between 320°C and 465°C, one between 465°C and 510°C, and two peaks between 510°C and 620°C. Additionally, one very minor, possibly insignificant peak is observed between 635°C and 665°C.

XRD analyses of all three reacted samples (see Figure 4. XRD analyses. (a) Starting material 25/5 1/M1, reacted material AS-P-01, and reacted material AS-P-01 after TGA. (b) Starting material 25/5 1/M1, reacted materials AS-P-01, RN-P-01, RN-P-02 and RN-P-07. (c) starting material 25/5 1/M4 and reacted materials RN-P-03, RN-P-09, RN-P-10, RN-P-11 and RN-P-12.b) did not show any change in the XRD-spectra compared to the starting material. Note that samples RN-P-01 and RN-P-01 were only analyzed for 2θ angles greater than 20°, meaning that potential changes in the spacing of the swelling clay minerals would not be observed. Sample RN-P-07 was analyzed over a 2θ range of 2 to 60°, with the analysis starting within 20 minutes after releasing the CO_2-pressure, and yet no peak shifts or other changes in the XRD-spectrum were observed. The new peak observed in sample AS-P-01 at ~43° was not observed in any of these samples.

3.3.2   Powder experiments on 25/5 1/M4

Six additional powder experiments were carried out on a ball-milled sample of shale 25/5 1/M4 (RN-P-03) or on micronized 25/5 1/M4 (RN-P-08 – RN-P-12). This particular shale sample was selected for its relatively high clay content.

After the first experiment, no clear changes were seen in the color or consistency of the powder. Degassing did result in the sample being distributed throughout the vessel, and about 0.9842 g of the initial 1.0000 g was recovered. After another 10 minutes, this recovered mass had decreased further to 0.9764 g through degassing of the powder.

TGA analysis on the reacted powder (Figure 3. TG Analyses performed on the Netzsch TGA, showing (a) a plot of remaining sample mass (%) vs. temperature (°C), and (b) a plot of the rate of mass loss (%/min) vs. temperature (°C), for the 25/5 1/M4 starting material, and samples exposed to supercritical CO2 or argon in experiments RN-P-03, RN-P-09, RN-P-10, RN-P-11 and RN-P-12.) showed little change overall relative to the starting material. There

was a slight increase in mass loss at lower temperatures, between 100°C and 200°C. Furthermore, a minor peak in the mass loss rate was observed between 220°C and 255°C. The main peak observed between 330°C and 480°C had not changed significantly. Finally, the mass loss rate measured at higher temperatures (around 600°C and between 700°C and 800°C) is slightly lower. A comparison of the XRD analyses of the starting material and the reacted powder showed no significant changes (see Figure 4. XRD analyses. (a) Starting material 25/5 1/M1, reacted material AS-P-01, and reacted material AS-P-01 after TGA. (b) Starting material 25/5 1/M1, reacted materials AS-P-01, RN-P-01, RN-P-02 and RN-P-07. (c) starting material 25/5 1/M4 and reacted materials RN-P-03, RN-P-09, RN-P-10, RN-P-11 and RN-P-12.c).

Experiment RN-P-08 was carried out on 0.9985 gr micronized 25/5 1/M4, using wet supercritical CO_2. Wet CO_2 was obtained by adding 5.9 gr demineralized water to the batch vessel. The water was kept separate from the sample by loading the powdered sample into a small titanium pot, which was in turn placed inside the vessel. A lid was placed on this pot. Access of CO_2 to the sample powder was ensured through a small hole in the lid, and through openings along the edge of the lid, which did not fully seal onto the pot.

After the experiment, 1.0351 gr powder was retrieved from the small pot. The small increase in mass was most likely caused by water uptake by the reacted powder. TGA and XRD analysis carried out on the powders after the experiment did not show any significant changes compared to the starting material (though some effects were observed in the TGA at low temperature, likely due to some apparatus settling, causing an artifact in the data see Figure 3. TG Analyses performed on the Netzsch TGA, showing (a) a plot of remaining sample mass (%) vs. temperature (°C), and (b) a plot of the rate of mass loss (%/min) vs. temperature (°C), for the 25/5 1/M4 starting material, and samples exposed to supercritical CO2 or argon in experiments RN-P-03, RN-P-09, RN-P-10, RN-P-11 and RN-P-12.).

Experiment RN-P-09 was carried out on 0.9990 gr of micronized 25/5 1/M4 powder, using supercritical CO_2 at 40°C and 10 MPa. However, in this experiment a Teflon-coated magnetic stirring rod was added to the batch vessel and the powder was continuously stirred during the experiment. After the experiment, the powdered sample was found in a caked layer on the wall and bottom of the vessel. The amount of powder retrieved was 0.9380 gr, but not all powder was retrievable.

XRD analysis showed no significant change to the sample compared to the starting material. However, a significant change was observed in the TGA carried out on this sample. As shown in Figure 4. XRD analyses. (a) Starting material 25/5 1/M1, reacted material AS-P-01, and reacted material AS-P-01 after TGA. (b) Starting material 25/5 1/M1, reacted materials AS-P-01, RN-P-01, RN-P-02 and RN-P-07. (c) starting material 25/5 1/M4 and reacted materials RN-P-03, RN-P-09, RN-P-10, RN-P-11 and RN-P-12.c, the start of the mass loss peak has shifted from ~350°C to 315°C. Furthermore, the originally sharp single peak has split into a wider and lower double peak, which disappears at about 580°C rather than 550°C.

Experiment RN-P-10 was carried out on 0.9993 gr micronized 25/5 1/M4 with supercritical CO_2 at a temperature of 80°C rather than 40°C. The sample was loaded inside a titanium pot placed in the vessel to help sample retrieval. Access of CO_2 to the sample was again ensured by a small hole in the lid on this pot, and along the edge of the lid, while during depressurization sample powder would be kept inside the pot. After the experiment, 1.0007 gr of sample was retrieved in the pot. XRD analysis and TGA showed no significant changes compared to the starting material.

In experiment RN-P-11, 1.0744 gr of micronized 25/5 1/M4 was reacted with Argon at 40°C and a pressure of 10 MPa, while stirring with a Teflon-coated magnetic stirring rod. After this experiment, 1.0725 gr of powder was retrieved from the vessel. While the powder did not form a thick caked layer on the wall and bottom of the vessel, the powder did appear to clump more than before.

Interestingly, XRD analysis showed the appearance of a minor peak at ~18° (4,9Å). In the TGA, similar changes were observed as for sample RN-P-09. The mass loss rate peak started at a lower temperature than observed for the unreacted sample (at ~315°C). Furthermore, the main mass loss peak observed in the starting material had again split into two separate peaks, and the second peak disappeared at a temperature of ~600°C. Compared to experiment RN-P-09 both peaks had shifted to slightly higher temperatures (the first peak from 375°C to 390°C, and the second from 480°C to 530°C).

A final experiment, RN-P-12, was carried out to test whether the presence of the Teflon coating on the stirring rod influenced the observed changes to the shale samples. In this experiment, a non-Teflon-coated, commercially available rare earth magnet was added to the vessel. Inspection of the sample after the experiment showed a black discoloration of the sample. Furthermore, the sample had strongly caked together, and some of the powder was magnetic. The discoloration and magnetic nature of the powder were most likely caused by erosion and chemical reaction of the magnet used to stir the sample, as the edges of the magnet had become rounded and the protective coating had partly disappeared. The sample mass retrieved was 1.3343 gr out of a starting mass of 0.9995 gr.

Significant changes to the powder were observed in TGA, with increased mass loss below 350°C, and a much reduced peak in mass loss rate between 320 and 465°C. Significant changes were also observed in the XRD, with the appearance of a new diffraction peak at 43,4°. Note that the high signal to noise ratio in this analysis is most likely caused by Fe fluorescence.

3.3.3   Block experiments RN-B-04, RN-B-05, RN-B-06, and RN-B-13

Four experiments were performed on intact blocks of shale. Experiments RN-B-04 and RN-B-05 were performed on 1.1 – 1.2 cm^3 blocks (dimensions between 8.5 and 13.6 mm) of 25/5 1/M4, with a duration of either 1 or 2 weeks. The aim was to determine whether interaction with supercritical CO_2 would result in drying out and splitting of the samples. Experiment RN-B-06 was performed using one cm-scale block of 25/5 1/M1 and one cm-scale block of 25/5 1/M9 in an attempt to reproduce the results reported by [8] (see also 3.2.2). Note that upon ending these experiments the pressure was released slowly to prevent any physical effects on the samples resulting from rapid depressurization. Experiment RN-B-13 was performed on a large (~5 cm^3) block of 25/5 1/M4 that was soaked in demineralized water for 24 hours before the experiment was started. The aim of this experiment was to study whether the removal of absorbed water from the sample due to interaction with supercritical CO_2 (especially the removal of water from smectite interlayer spacings) could result in cracking of the sample. Furthermore, at the end of this experiment, the pressure was released rapidly (within 1 minute).

Upon opening the vessel after experiment RN-B-04 and RN-B-05, changes in the sample blocks were not observed optically. Measurements of the sample mass executed after opening the vessel showed that both samples had increased in mass (from 2.529 g to 2.538 g and from 2.8930 g to 2.9030 g, respectively, for experiment RN-B-04 and RN-B-05). Note

that in the case of experiment RN-B-05 this mass was determined several hours after the CO_2-pressure was released. Furthermore, measurements of sample Rn-B-05 implied a 1% increase in height (i.e. perpendicular to the layering), though exact measurement of this dimension was difficult as the sample was not perfectly flat. One week after ending experiment RN-B-04, the sample mass had decreased to 2.525 g, i.e. lower than the starting mass. Eight days after ending experiment RN-B-05, this sample had decreased to 2.893 g, i.e. close to its initial mass.

Upon opening the vessel after experiment RN-B-06 no effluence of fluids was observed from either sample. Furthermore, both samples had remained intact and did not look particularly dried out. The masses of both samples had increased. The mass of the 25/5 1/M1 sample had increased from 6.052 to 6.146 g immediately upon opening the vessel (roughly 5 minutes after releasing the CO_2-pressure). The mass of the 25/5 1/M9 sample had increased from 5.537 g to 5.559 g. Fifteen minutes after releasing the pressure the masses of the sample blocks had decreased to 6.091 g and 5.557 g, respectively. Furthermore, after opening the vessel it was noted that sample 25/5 1/M1 produced soft but audible pops, particularly on its top and bottom surfaces (i.e. on its bedding planes. Neither sample showed any appreciable increase in size perpendicular to the layering.

After experiment RN-B-13, the shale sample block appeared dry. The sample dimensions were similar to those of the wet sample before the experiment, but the sample mass had decreased to 11.4285 g (from 11.4439 g). Furthermore, five bedding-parallel (or near-parallel) cracks were observed along the surface of the sample. With only a little effort, the sample pulled apart along these cracks, indicating little residual splitting strength.

4 Discussion and comparison of results

Two series of experiments were carried out in which samples of shale were directly exposed to CO_2 in supercritical or near-supercritical state. Both the starting materials, and the resulting products were analyzed using optical methods, TGA and XRD. Here we will interpret and discuss the results of these experiments.

4.1 Starting materials

XRD and TG Analyses were carried out in order to determine whether changes in the composition of the powdered shale samples had occurred during experiments in which this shale was exposed to CO_2. Quantification of the starting material composition had already been carried out (see [9]), and the compositions of the used materials are given in **Table 1**. Shale compositions..

Based on the reported sample composition, the thermally active phases in the starting material 25/5 1/M1 are clay minerals (kaolinite, smectite, illite), carbonates (especially dolomite/ankerite, but also calcite and siderite) pyrite and organic carbon. The removal of adsorbed and interlayer water can explain any mass loss observed in the TGA at low temperature (up to ~200°C – see [10]). Dehydroxylation of the different clay materials occurs at 530°C-590°C (kaolinite), ~550°C (illite) and ~700°C (montmorillonite – [10]). Based on the reported mineral contents, these dehydroxylation reactions could result in a mass loss of about 1.2%, in the temperature range above 530°C mainly due to kaolinite dehydroxylation. A major thermally active component is pyrite, which under anoxic conditions may disproportionate at ~600-700°C[10]. Such disproportionation of the 22% pyrite (FeS_2) contained in the sample to pyrrhotite ($Fe_{0.95}S_{1.05}$) could explain a mass loss of ~5.3% if the sulfur released evaporates. Finally, at temperatures above 540°C, decarbonation of siderite (540-555°C), ankerite (650-700°C), dolomite (750-800°C) and calcite (895°C) occurs.

A plot of the mass loss rate vs. temperature as measured for sample 25/5 1/M1 is given in Figure 2. TG Analyses performed on the Netzsch TGA, showing (a) a plot of remaining sample mass (%) vs. temperature (°C), and (b) a plot of the rate of mass loss (%/min) vs. temperature (°C), for the 25/5 1/M1 starting material, and samples exposed to (near-)supercritical CO2 in experiments AS-P-01 and RN-P-07.b. A double peak is observed at low temperature (below 140°C, resulting from the evaporation of surface-adsorbed water. A major double mass loss peak is measured between 320°C and 510°C, with the main peak around 415°C. Another, smaller peak is observed between 510°C and 620°C. The observed mass loss between 510°C and 620°C, over which interval 1.9% mass is lost, is most likely the result of dehydroxylation of kaolinite and illite, and decarbonation of siderite. However, the above thermal reactions do not explain the observed ~6.5% mass loss between 320°C and 510°C. Mass loss in this temperature range is most likely the caused by the pyrolysis of hydrocarbons (see for example [11]), as sample 25/5 1/M1 contains about 6.2% organic carbon. This suggests that the expected mass loss due to pyrite disproportionation did not occur. XRD analysis on a sample after TG Analysis showed that the previously observed pyrite diffraction peaks no longer occurred, while new peaks were observed that may be attributed to pyrrhotite. This indicates that some pyrite disproportionation likely did occur, but that the total pyrite content may have been lower than the indicated 22%[9], or that the released sulfur was not lost from the sample.

The TG Analysis of sample 25/5 1/M4 (see Figure 3. TG Analyses performed on the Netzsch TGA, showing (a) a plot of remaining sample mass (%) vs. temperature (°C), and (b) a plot of the rate of mass loss (%/min) vs. temperature (°C), for the 25/5 1/M4 starting material, and samples exposed to supercritical CO2 or argon in experiments RN-P-03, RN-P-09, RN-P-10, RN-P-11 and RN-P-12.b) shows dehydration at temperatures below 130°C. Then, a large peak in mass loss rate is observed between 330°C and 480°C, where 8.5% mass is lost. As discussed for sample 25/5 1/M1, this peak is most likely related to hydrocarbon pyrolysis. Ongoing mass loss between 480°C and 700°C (3.9%) would is then explained by kaolinite and illite dehydroxylation along with siderite decarbonation. Mass loss between 600 and 700°C can additionally be related to pyrite disproportionation. The minor peak in the mass loss rate observed above 700°C (~1.5% mass lost) can most likely be ascribed to further decarbonation reactions and/or montmorillonite dehydroxylation.

4.2 Preliminary experiments

Two initial experiments were carried out in 2013 and reported by Souche [8]. In experiment AS-P-01, micronized shale sample 25/5 1/M1 was exposed to CO_2 at 30°C and 70 Bar. After the experiment, the powder had agglomerated, and was reported to be somewhat lighter in color.

Compared to the starting material, the reacted sample showed a more constant rate of mass loss in the TGA, though small variations in this rate are visible, coinciding with the variations measured on the starting material. Both repeat analyses (performed over a year after the initial analysis) show a similar mass loss curve. This indicates that the change induced in the sample during the experiment is permanent in nature.

The mass loss rate curve (displayed in Figure 2. TG Analyses performed on the Netzsch TGA, showing (a) a plot of remaining sample mass (%) vs. temperature (°C), and (b) a plot of the rate of mass loss (%/min) vs. temperature (°C), for the 25/5 1/M1 starting material, and samples exposed to (near-)supercritical CO2 in experiments AS-P-01 and RN-P-07.b) shows peaks between 70°C and 120°C, between 320°C and 445°C, and between 445°C and 600°C, and a minor peak between 625°C and 715°C. Compared to the starting material, the two peaks between 320°C and 600°C have a significantly decreased intensity, and have shifted to somewhat lower temperature, while the peak between 510°C and 620°C has disappeared, and a new peak was observed between 625°C and 715°C. The changes to the peaks between 320°C and 600°C suggest that a change may have occurred to both the content and the composition of the hydrocarbons contained in the sample. A change to the hydrocarbons might also explain the increased continuous mass loss observed at low temperatures. Such a change would not be observed in XRD analysis. The new peak observed between 625°C and 715°C is very minor, but is possibly related to the decarbonation of some (~1.4%) ankerite that may have formed during the experiment. The disappearance of the mass loss peaks between 510°C and 620°C likely reflects changes to the thermally active minerals (kaolinite, illite) in the starting material.

The XRD analysis of the reacted sample did not show a shift in the reflectance peaks. However, a significant new peak was observed at ~43°. This peak was also observed in a recent re-analysis of the reacted sample, demonstrating that the change to the sample was not transient in nature. A permanent change in the mineralogy of the sample has thus occurred during the experiment, or after that. It is currently not known what caused this change. One possible reaction is the carbonation of pyrite. However, the peaks observed in the XRD related to pyrite do not disappear between the analyses performed on the starting

material and on the reacted powder. Hence, if carbonation of pyrite occurred, this did not result in significant removal of the pyrite during the experiment. Another possible explanation is the addition of corundum (Al_2O_3) to the sample, which may have been added as an internal reference or pollution may have occurred accidentally. However, the addition of Corundum to our sample would not explain all changes observed in the TGA. Furthermore, the XRD analysis performed on a sample that has been treated in the TGA shows that the phase causing the peak was not stable. Hence, it seems unlikely that corundum caused the 43° diffraction peak observed in sample AS-P-01.

In experiment AS-B-02, two cm-scale blocks of shale were reacted with liquid CO_2 under near-supercritical conditions (30°C and 7.5 MPa). After the experiment, the piece of 25/5 1/M1 shale appeared dried out, and had split along several of its layers. The piece of 25/5 1/M9 shale remained intact and still appeared wet. Furthermore, fluids were being expelled from this shale block. Analysis showed these fluids to be rich in hydrocarbons. This suggests that contact with CO_2 resulted in removal of water from the piece of M1-shale, including interlayer water from swelling clays, and in the mobilization of hydrocarbons in the piece of M9-shale.

4.3   Second series of experiments

Experiments RN-P-01 and RN-P-02 were performed in an attempt to reproduce the results of [8]. However, TGA and XRD analyses performed within a few hours after the experiments were ended showed no significant change to the samples. The mass losses measured during TG Analyses were similar to those of the starting materials, and the XRD spectra showed no clear changes in the measured 2θ range (20°-70°).

A third experiment (RN-P-07) was performed on the same sample, and under similar conditions, but with the addition of a small amount of water. The TG Analysis of the reacted sample showed a very similar mass loss pattern to that of the starting material. However, increased mass loss was observed at low temperature (<100°C), likely related to ongoing degassing and drying of the sample. Furthermore, an additional minor mass loss peak was observed between 635°C and 655°C. A possible explanation for this peak is the decarbonation of a minor amount of ankerite and/or siderite (~0,5%). The XRD spectrum of sample RN-P-07 showed no significant change compared to the starting material, though very small amounts of newly-formed minerals would likely not be observed.

These three experiments therefore did not show any reactions occurring to the 25/5 1/M1 shale, in contrast to the preliminary experiments reported by [8]. Here, we will consider possible interactions that would be expected to take place. XRD analysis of the 25/5 1/M1 starting material showed diffraction peaks caused by clay minerals at 7 and at 10 Å (and possibly a very minor, broad peak around 14 Å). The peak at 7 Å can be attributed to kaolinite. The peak at 10 Å can most likely be attributed to either illite, or dehydrated smectite (with no interlayer water – e.g. see [7]). The reflection peak at 14Å may represent hydrated smectite with 2 water layers (2W). Shifts in clay peaks have been observed for swelling clays (smectites) due to interaction with CO_2, as CO_2 either removes water from the interlayer space causing contraction (from hydrated clays with at least 2 planes of interlayer H_2O molecules, 2W, see [5], or due to intercalation of CO_2 in partially hydrated smectites (1W) causing swelling (see [5]). Completely dehydrated smectite shows only very slight swelling when exposed to CO_2 ([7]). Based on the XRD analysis, a very minor amount of smectite with 2W hydration state may have been present in our 25/5 1/M1 starting materials. During the experiments, reaction with CO_2 might have caused this smectite to dehydrate and

contract. However, such an effect would most likely be transient in nature, with rehydration of the smectite occurring when the sample is exposed to (moist) air. If any swelling of dehydrated smectite occurred due to intercalation of CO_2, this effect would likewise have been very limited and very transient in nature. Swelling or contraction of smectite due to interaction with CO_2 can therefore probably only be observed using in-situ methods. Other interactions, including more permanent chemical reactions, due to exposure of the mineral phases present in our samples to dry supercritical CO_2 are not expected to occur. Our observations that no reactions that are observable after the experiment occur when powdered shale is exposed to (dry) supercritical CO_2 are thus in line with expectation, and with experiments such as those reported by Credoz et al [4].

Additional powder experiments were carried out on shale sample 25/5 1/M4. Comparison of the analyses performed on this starting material and on the reaction products RN-P-03 and RN-P-10 (carried out at 80°C) showed no significant changes in either the TG Analysis or the XRD patterns. However, in experiment RN-P-09, a magnetic stirring rod was used to agitate the powder sample. While again no changes were observed to the sample in XRD, significant changes were observed in the TG Analyses, where a single peak observed for the starting material between 350°C and 550°C had been replaced by a lower double peak between 315°C and 580°C. As discussed above, these changes likely represent a change to the hydrocarbon content of the reacted samples.

The main function of stirring in chemical experiments is to assure homogeneity in the composition of the fluid phase, around reacting grains. This can limit the effect of concentration build up around such grains when diffusion is slow, thus enhancing overall reaction kinetics. To investigate whether the homogenization of the composition of the CO_2 phase was the main reason a reaction was observed in the stirred experiments, experiment RN-P-11 was performed using Argon instead of CO_2. Here, similar changes were observed in the TGA as were observed for experiment RN-P-09, showing that these changes occurred irrespective of whether CO_2 was present, and excluding any chemical or other effect of CO_2 on the hydrocarbons contained in the sample. The new diffraction peak observed in the XRD at 18° is not explained.

As the effects observed in the TGA (changes to the hydrocarbons contained in our powdered shale samples) were caused by the presence of a magnetic stirring rod, a final powder test was carried out to determine whether the effect was related to the mechanical action of the rod, or to any possible effects related to the Teflon coating. In this experiment, a commercially available magnetic rod without Teflon coating was used. Very significant effects were again observed in the TGA. Here, a significant change to the mass loss peak around 425°C is again interpreted as a change to the kerogen contained in the sample. This then means that these changes were not related to the presence of the Teflon coating on the stirring rod. Additional changes observed in the TGA are likely the result of the chemical interaction between the magnet and the CO_2, as well as erosion of the magnet, as suggested by optical observations. We thus conclude that the changes to the shale kerogen observed in a number of our experiments were caused by a mechanical effect induced by the continuous grinding movement of the magnetic stirring rod in the experiments in which such a rod was applied. Furthermore, a new peak was observed in the XRD around 43.4°. This can also be ascribed to chemical interaction between the magnet and the CO_2.

Further experiments were performed on intact pieces of shale rock (RN-B-04, RN-B-05, RN-B-06 and RN-B-13). After these experiments, only optical observations and mass measurements were performed to determine if interaction with dry supercritical CO_2 resulted in any changes in these rocks. After ending experiments RN-B-04 and RN-B-05 (performed on 1.1 – 1.2 cm^3 cuboids of 25/5 1/M4), only slight (~0.4%) increases in mass were observed

on the samples within hours after the pressure was released. These increases in mass can most likely be attributed to CO_2-uptake into the rock microstructure (in the pore network, and in clay minerals). This uptake of CO_2 may have resulted in minor swelling but precise measurement of the dimensions of the used samples was problematic due to the uneven sample shapes. One week after the experiments, the sample masses had returned to its initial value, or to a slightly lower value. This subsequent decrease back to the initial sample mass then resulted from diffusion of CO_2 out of the sample. The decrease of the mass of one sample to just below the initial mass suggests some removal of fluids (water and/or hydrocarbons) may have taken place. No other effects of exposure to supercritical CO_2 were observed.

The sample blocks exposed to CO_2 in experiment RN-B-06 likewise remained largely unaltered. The 25/5 1/M1 and 25/5 1/M9 samples, respectively, showed ~1.6% and 0.4% increases in mass (measured roughly 5 minutes after releasing the CO_2-pressure), likely resulting from CO_2-uptake. Neither sample showed any significant swelling due to this CO_2 uptake, though. Interestingly, the 25/5 1/M1 sample produced soft audible pops on its top and bottom surfaces (i.e. bedding planes), which most likely resulted from the release of over-pressurized CO_2 from inside the sample.

After experiment RN-B-13, the sample block of 25/5 1/M4 shale that had been saturated with demineralized water before being exposed to supercitcial CO_2 (RN-B-13) did show bedding-parallel cracking, and came apart easily along those cracks. Furthermore, the sample appeared dried, and the sample mass had decreased relative to its water-saturated mass before exposure to CO_2. (Unfortunately, the dry sample mass before water-saturation was not determined.) This suggests that most effects observed in the preliminary block experiment (AS-B-02) may have been caused by removal of water from the samples due to exposure to dry supercritical CO_2 rather than any chemical effects that this CO_2 might have had. As discussed above (see also [5][6][7]), such removal of interlayer water from swelling clays (smectite) will result in shrinkage of the clay minerals, which in turn can induce cracking in shale samples.

4.4 Comparison of preliminary and later experiments

The preliminary powder experiment reported by Souche [8], a micronized shale sample was reacted with CO_2 at near-supercritical conditions (7 MPa and 30°C). After this experiment, Souche observed changes to the sample in the TGA, which were interpreted as changes to the shale sample's kerogen content, and the appearance of a new peak in the XRD at ~43°. In our second series of experiments, it was attempted reproduce and further research these results. It was found that the changes observed in the TGA could only be reproduced if, during the experiment, the sample was agitated using a magnetic stirring rod. Furthermore, the results were also reproduced when using Argon instead of CO_2. Therefore, it was concluded that the effect resulted from the smearing effect of the stirring rod, rather than from a chemical effect induced by the CO_2.

The appearance of a (minor but significant) new diffraction peak in the XRD could not be reproduced. Furthermore, no good explanation was found for the appearance of this peak. It is possible that this change was not an effect of reaction with CO_2, but represents pollution of the sample.

Souche [8] further reported an experiment in which cm-scale blocks of shale were exposed to near-supercritical CO_2 at 7.5 MPa and 30°C. After these experiments, he observed that

one shale block appeared dry, and had split in several places, parallel to the bedding. The second (25/5 1/M0, which had a higher organic carbon content) still appeared "wet" and was expelling fluids that analysis showed to be hydrocarbon-bearing. Experiments carried out on similar blocks of shale that had been stored in air over extended periods of time, and could be considered dry, did not show these effects. Drying and cracking along bedding was observed in one experiment, performed on a block of 25/5 1/M4 shale that had been pre-soaked in water before the experiment was started. Here, it was concluded that the observed effects were most likely related to the removal of water from wet shale. Exposure to supercritical CO_2 lead to the removal of interlayer water from swelling clays, which resulted in shrinkage and cracking.

While most effects reported by Souche [8] have now been re-produced and explained, some minor effects were not. However, considering the limited amount of information available about the preliminary experiments, it was decided not to proceed further with investigating this. Especially the potential hydrocarbon release from (a wet) shale sample block 25/5 1/M9 could be of interest for future research. However, it is advised to carry out such future experiments on freshly sampled shales.

5 Conclusions and suggestions for future work

- Exposure of micronized shale to (supercritical) CO_2 at ~7-10 MPa and 30-80°C was shown to result in the changes in the sample kerogen content, apparent in TGA as a splitting of the main mass loss peak (caused by kerogen pyrolysis) into two peaks. However, these changes only occurred if during the experiment the sample was agitated using a magnetic stirring rod.

- Another experiment, at 10 MPa and 40°C, but using argon rather than CO_2, showed similar effects, indicating that the observed effect was caused by the magnetic stirring rod, and was not related to the exposure to CO_2. A further experiment using a commercially available magnet that was not Teflon-coated showed similar effects indicating that the effect was caused by the physical action of the stirring magnet on the sample.

- During preliminary experiments, in XRD analysis of the sample after testing, a new diffraction peak was observed at 43°. After the argon experiment, a new diffraction peak was observed at 18°. These changes to the samples were not explained.

- Experiments on cm-scale blocks of shale showed that exposure of shale to (supercritical) CO_2 at 30-40°C and 7-10 MPa resulted in the samples drying out and cracking along bedding. However, these effects were only observed if the sample contained some water before the experiment was started. Experiments carried out on air-dried samples did not show such effects.

- During the preliminary experiments, one sample block still appeared wet after the experiment, and was expelling a hydrocarbon-bearing fluid. This experiment was not reproduced, but no experiments were carried out on a pre-soaked sample of this shale (which had a higher organic carbon content).

- If future experiments on the exposure of shale to supercritical CO_2 are performed, the use of fresh samples which still contain their original fluids is advisable. For the observation of some of the effects of exposure to CO_2 that can be expected to occur, however, in-situ measurement techniques would be required (cf.[5][6][7]).

6 References

[1] Alemu, B.L.; P. Aagaard; I.A. Munz; E. Skurtveit (2011) Caprock interaction with CO_2: A laboratory study of reactivity of shale with supercritical CO_2 and brine. *Appl. Geochem. 26*, 1975-1989.

[2] Bateman, K.; C.A. Rochelle; G. Purser; S.J. Kemp; D. Wagner (2013) Geochemical interactions between CO_2 and minerals within the Utsira caprock: A 5-year experimental study, *Energy Procedia 37*, 5307-5314.

[3] Kaszuba, J.P.; D.R. Janecky; M.G. Snow (2005) Experimental evaluation of mixed fluid reactions between supercritical carbon dioxide and NaCl brine: Relevance to the integrity of a geologic carbon repository. *Chem. Geol. 217*, 277-293.

[4] Credoz, A.; O. Bildstein; M. Jullien; J. Raynal; J.-C. P'etronin; M. Lillo; C. Pozo and G. Geniaut (2009) Experimental and modeling study of geochemical reactivity between clayey caprocks and CO2 in geological storage conditions, *Energy procedia*, 3445-3542.

[5] Schaef, H.T.; E.S. Ilton; O. Qafoku; P.F. Martin; A.R. Felmy and K.M. Rosso (2012) In situ XRD study of Ca^{2+} saturated montmorillonite (STX-1) exposed to anhydrous and wet supercritical carbon dioxide. *Int. J. Greenh. Gas Con.* 24, 149-161, doi:10.1016/j.ijggc.2011.11.001.

[6] Ilton, E.S.; H.T. Schaef; O. Qafoku; K.M. Rosso and A.R. Felmy (2012) In Situ X-ray Diffraction study of Na^+ saturated montmorillonite exposed to variably wet super critical CO_2. *Environ. Sci. Technol.* 46, 4241-4248, doi:10.1021/es300234v.

[7] De Jong, S.M.; C.J. Spiers and A. Busch (2014) Development of swelling strain in smectite clays through exposure to carbon dioxide. *Int. J. Greenh. Gas Con.* 24, 149-161, doi:10.1016/j.ijggc.2014.03.010.

[8] Souche, A. (2013) Clay dehydration experiments. IFE Internal report.

[9] Iden, K. (1992) Mudrock diagenesis and synthesis on mudrock-sandstone diagenetic interaction. Results from the inorganic part of the data acquisition (activity 1) in project EAN 1584: Porosity and permeability prediction modelling. IFE internal report, EAN 1584.

[10] Földvári, M. (2011) Handbook of thermogravimetric system of mineral and its use in geological practice. Occasional Papers of the Geological Institute of Hungary, volume 213.

[11] Tiwari, P. and M. Deo (2012) Compositional and kinetic analysis of oil shale pyrolysis using TGA-MS. *Fuel* 94, 333-341, doi:10.1016/j.fuel.2011.09.018.